ISSN 1063-7834, Physics of the Solid State, 2016, Vol. 58, No. 8, pp. 1521–1527. © Pleiades Publishing, Ltd., 2016.
Original Russian Text © A.Yu. Stroeva, V.P. Gorelov, A.V. Kuz'min, 2016, published in Fizika Tverdogo Tela, 2016, Vol. 58, No. 8, pp. 1473–1478.

SEMICONDUCTORS

# Conductivity of Perovskites $La_{0.9}Sr_{0.1}Sc_{1-x}Fe_xO_{3-\alpha}$ ($x = 0.003–0.47$) in Oxidizing and Reducing Atmospheres

**A. Yu. Stroeva[a, *], V. P. Gorelov[a], and A. V. Kuz'min[a, b]**

[a] *Institute of High-Temperature Electrochemistry, Ural Branch of the Russian Academy of Sciences, ul. Akademicheskaya 20, Yekaterinburg, 620137 Russia*

[b] *Ural Federal University named after the first President of Russia B.N. Yeltsin, ul. Mira 19, Yekaterinburg, 620002 Russia*

**e-mail: stroevaanna@yandex.ru*

Received December 8, 2015; in final form, January 30, 2016

**Abstract**—The conductivity of single-phase ceramic materials based on proton-conducting perovskite $La_{0.9}Sr_{0.1}ScO_{3-\alpha}$ containing from 0.3 to 47 at % Fe in the scandium sublattice has been studied. Synthesis has been performed by burning with ethylene glycol. Measurements have been carried out by the four-probe (500–900°C) and impedance (100–500°C) methods in oxidizing and reducing atmospheres, as well as at different pressures $p_{O_2}$ ($2.1 \times 10^4$–$10^{-15}$ Pa) and $p_{H_2O}$ (0.04–2.5 kPa). Substitution of scandium with iron significantly decreases the proton conductivity.

**DOI:** 10.1134/S1063783416080278

## 1. INTRODUCTION

Fuel cells, including extensively studied solid-oxide fuel cells (SOFCs), allow efficient direct chemical to electric energy conversion. For SOFC developments directed to a decrease in operating temperatures, high-conductivity solid electrolytes are required in addition to active electrodes. Oxide proton electrolytes with perovskite structure, among which are electrolytes based on $LaScO_3$, are most promising for this purpose, taking into account their high bulk conductivity at lower temperatures [1, 2]. However, efficient application of these materials requires finding methods for decreasing their higher grain-boundary resistance whose causes are not readily apparent. One of the simple ways of solving this problem is the introduction of modifying additives, in particular, iron oxide [3, 4]. In this case, small iron oxide additives promoting the formation of dense boundaries could lower grain-boundary resistances of proton electrolyte; large additives could transform these materials to membranes with proton–electron conductivity [5], which is also an important problem.

The highest bulk conductivity among materials based on $LaScO_3$ is observed in the $La_{1-y}Sr_yScO_{3-\alpha}$ system at $y = 0.10$ [6]. Proton electrolytes and membranes are used in both oxidizing and reducing media; therefore, the objective of this work is to study the effect of iron cations in the scandium sublattice on electromigration in ceramic materials $La_{0.9}Sr_{0.1}Sc_{1-x}Fe_xO_{3-\alpha}$ (LSSF) ($x = 0.003$–$0.47$) in a wide oxygen pressure $p_{O_2}$ range.

This study continues the cycle of our works [6–12] on the study of properties of proton-conducting oxides based on $LaScO_3$.

## 2. EXPERIMENTAL TECHNIQUE

### 2.1. Synthesis of $La_{0.9}Sr_{0.1}Sc_{1-x}Fe_xO_{3-\alpha}$ Samples

Ceramic samples of composition $La_{0.9}Sr_{0.1}Sc_{1-x}Fe_xO_{3-\alpha}$ (hereafter, LSSF0.3, LSSF0.6, LSSF1.6, and so on) were synthesized by burning with ethylene glycol. As starting materials, we used lanthanum oxide, scandium oxide, strontium carbonate (no lower than chemically pure grade), and carbonyl iron, which were dissolved in nitric acid. A mixture of solutions taken in the required ratio calculated for 10 g of product was evaporated to a volume of ~50 mL and ~5 mL ethylene glycol was added. After self-ignition, obtained powders were annealed at a temperature of 700°C for 1 h. Samples were pressed at 200 MPa and burned in air at a temperature of 1400°C (3 h) in a charge of $La_{0.9}Sr_{0.1}ScO_{3-\alpha}$ (LSS) powder.

An X-ray diffraction (XRD) analysis was performed in Cu$K_\alpha$ radiation using a Rigaku DMAX 2200 diffractometer with a monochromator.

### 2.2. Conductivity Measurements

These measurements were performed on samples with platinum electrodes by the four-probe and impedance spectroscopy methods. The four-probe method was used to measure the total conductivity using an automated setup in the range of 900–500°C in the mode of cooling with a step of 10°C; the exposure time at each temperature was 1 h. The data were also measured as functions of the oxygen pressure ($2.1 \times 10^4$–$10^{-15}$ Pa) and the water vapor pressure in air (0.04–2.35 kPa).

Impedance measurements of the conductivity of LSSF samples 0.9–1.2 mm thick, containing to 3 at % Fe, were performed using a Parstat 2273 electrochemical system in the temperature range of 500–100°C in the mode of cooling with a step of 50°C; the exposure time at each temperature was no less than 24 h. The frequency range of measurements was from 1 MHz to 0.1 Hz at the alternating voltage amplitude of 10–30 mV. The effective activation energies were determined by the temperature dependences of the conductivity using the modified Arrhenius equation $\sigma T = A\exp(E_{act}/kT)$.

The atmospheric moisture was set by air circulation through a bubbler with a controlled water temperature, and "dry" air ($p_{H_2O}$ = 0.04 kPa) was obtained by its circulation through a zeolite column. The oxygen activities $pO_2$ in the atmosphere were set and maintained by an automated regulator with an electrochemical oxygen pump based on YSZ ($0.9ZrO_2 + 0.1Y_2O_3$) solid electrolyte, and $p_{O_2}$ was measured by a potentiometric oxygen sensor.

## 3. RESULTS AND DISCUSSION

### 3.1. Model of LSSF Defects

When a fraction of lanthanum cations $La^{3+}$ are substituted with strontium cations $Sr^{2+}$ in $LaScO_3$, substitutional defects $Sr'_{La}$ and oxygen vacancies $V_O^{\bullet\bullet}$ (Kröger–Vink notation) appear,

$$SrO(-LaO_{1.5}) \rightarrow Sr'_{La} + 0.5V_O^{\bullet\bullet} + O_O^{\times}. \quad (1)$$

The interaction of water vapor with LSS results in the appearance of protons in oxide, according to the Wagner quasi-chemical reaction,

$$H_2O + V_O^{\bullet\bullet} = 2H_i^{\bullet} + O_O^{\times}. \quad (2)$$

In an oxidizing atmosphere, the reaction leading to the formation of electron holes $h^{\bullet}$ in oxide occurs,

$$\frac{1}{2}O_2 + V_O^{\bullet\bullet} = 2h^{\bullet} + O_O^{\times}. \quad (3)$$

In reducing atmospheres, LSS loses oxygen, which results in an increase in the *n*-type electronic conductivity,

$$O_O^{\times} = V_O^{\bullet\bullet} + \frac{1}{2}O_2 + 2e'. \quad (4)$$

It is known that the perovskite lattice stabilizes the highest oxidation states of cations [13], which results in the appearance of $Fe^{4+}$ cations in LSSF. In [5] where LSSF materials containing ≥20 at % of Sr were studied, the dominant $Fe^{4+}$ content was confirmed by the titration method with KI. In our previous study [12], presence of iron with $Fe^{4+}$ oxidation state in the LSS + $FeO_{1.5}$ system was also confirmed by the Mössbauer method.

An increase in the iron oxidation state to 4+ results in a decrease in the concentration of oxygen vacancies by the reaction

$$2Fe_{Sc}^{\times} + V_O^{\bullet\bullet} + \frac{1}{2}O_2 = 2Fe_{Sc}^{\bullet} + O_O^{\times}. \quad (5)$$

At high iron cation contents in the form of $Fe^{3+}$ and $Fe^{4+}$ in LSSF, hole migration over chains ($-Fe^{4+}-O^{2-}-Fe^{3+}-$) is realized.

### 3.2. Sample Certification

The X-ray diffraction analysis showed that iron being a mineralogical analogue of scandium efficiently substitutes it in the entire range of studied additives (to 47 at % Fe) with the formation of single-phase LSSF solid solutions based on the orthorhombic perovskite-like structure. The data obtained are in agreement with the results of [5], whose authors first reported about the existence of the continuous region of solid solutions for LSSF, studied in the Fe concentration range of 0–100 at %, at Sr contents of 20 and 30 at %.

The unit cell volume decreases as iron is introduced (Fig. 1), as in [5], due to the smaller iron ion radius in comparison with scandium (according to Shannon [14], $r_{Sc^{3+}}$ = 0.745 Å, $r_{Fe^{3+}}$ = 0.55 Å, and $r_{Fe^{4+}}$ = 0.585 Å) for a coordination number of 6. The sample density was 90–96% of the theoretical one.

### 3.3. LSSF Impedance Measurements under Oxidizing Conditions

The impedance spectra measured in moist air contain semicircles corresponding to various relaxation processes. As an example, Fig. 2 shows the impedance loci for the LSSF3 sample, measured at temperatures of 350 and 400°C. In principle, the impedance locus can be divided into three parts (semicircles). The high-frequency spectral region (semicircle) characterizes the relaxation process associated with the electrolyte volume, the midfrequency semicircle characterizes the grain-boundary resistance, and the low-frequency

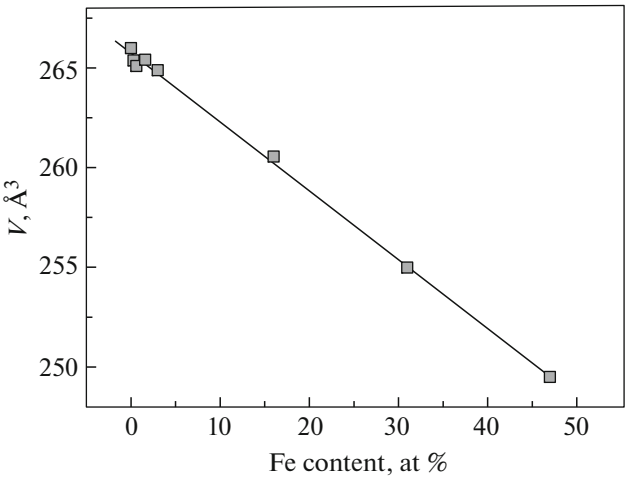


**Fig. 1.** Dependence of the LSSF unit cell volume on the iron content in the scandium sublattice.

hodograph locus region corresponds to the electrode process (the capacitance $C = 10^{-4}$–$10^{-5}$ F). In the present experiment, in the range of used frequencies, semicircles are observed, which are related to the processes at grain boundaries and at the electrode (Fig. 2). The intersection of the approximating semicircle with the horizontal axis (Fig. 2) allows the determination of the total $R_{tot}$, bulk $R_{bulk}$, and grain-boundary $R_{gh} = R_{tot} - R_{bulk}$ resistivities of the solid electrolyte.

As for the other materials based on $LaScO_3$ [7], the LSSF bulk conductivity appeared higher than the grain-boundary conductivity in the temperature range under study by 1.5–2 orders of magnitude (Fig. 3). Therefore, the total and grain-boundary conductivities slightly differ due to the overwhelming contribution of the grain-boundary resistivity to the total resistivity of samples. From these data, we can see the importance of the problem of grain-boundary resistivities for oxide proton electrolytes.

The temperature dependences of the LSSF bulk conductivity, measured in the range of 350–200°C exhibit substantially smaller slopes than the temperature dependences of grain-boundary conductivities (Fig. 3). The bulk conductivity activation energies can be considered as independent of composition (0.3–1.6 at % Fe) within the error and equal to 48 ± 1 kJ/mol.

### *3.4. LSSF Conductivity Measurements by the Four-Probe Method*

The temperature dependences of the LSSF total conductivity, measure by the four-probe method in air differ significantly for samples with small (Fig. 4a) and large (Fig. 4b) iron additives. The introduction of small (0.3–0.6 at % Fe) iron amounts (Fig. 4a; Fig. 5, inset) results in a decrease in the LSS conductivity and an increase in the activation energy; the introduction of large iron additives (above 3 at % Fe) leads to an increase in the conductivity (Fig. 5) at low activation energies (Fig. 4b). As a result, the conductivity isotherms (500–800°C) are shaped as curves with a minimum in both dry and moist air (Fig. 5).

The significant decrease in the activation energy and the increase in the LSSF conductivity at high iron concentrations indicate the change in the dominant conductivity mechanism which is implemented by hole transport over $(-Fe^{4+}-O^{2-}-Fe^{3+}-)$ chains as in lanthanum or strontium ferrites.

The symbasis of the conductivity isotherms in the $La_{0.9}Sr_{0.1}Sc_{1-x}Fe_xO_{3-\alpha}$ system under study and in the $(1-x)La_{0.9}Sr_{0.1}ScO_{3-\alpha} + xFeO_{1.5}$ system (at superstoichiometric iron oxide additives) [12] points to the identical mechanism of the effect of iron on the grain-boundary conductivity in both cases (Fig. 6). However, superstoichiometric doping causes scandium oxide to grain boundaries; therefore, the conductivity of such samples is lower than the conductivity of single-phase LSSF materials.

### *3.5. Effect of Air Humidity on the LSSF Total Conductivity*

According to reaction (2), an increase in air humidity leads to an increase in the proton concentration in oxide and to the proton conductivity. Experiments showed that the effect of air humidity on the

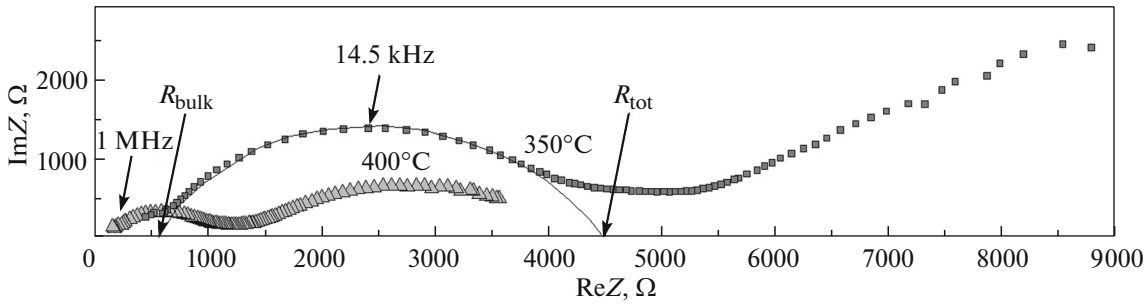


**Fig. 2.** Impedance loci for the LSSF3 sample at temperatures of 350 and 400°C in a moist air atmosphere at $p_{H_2O} = 2.35$ kPa.

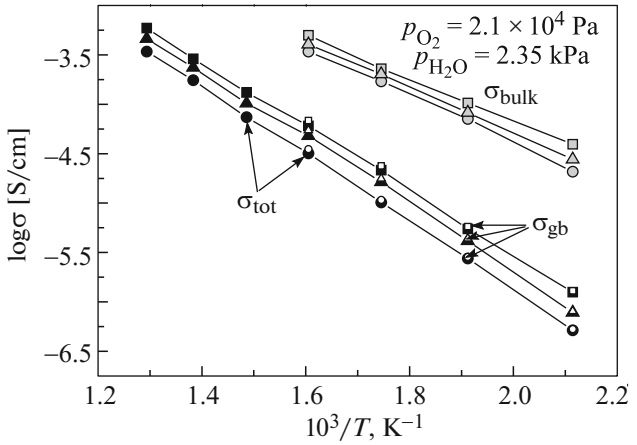


**Fig. 3.** Temperature dependences of the total (closed symbols), grain-boundary (open symbols), and bulk (gray symbols) conductivity of LSSF0.3 (squares), LSSF0.6 (circles), and LSSF1.6 (triangles) samples in a moist air atmosphere at $p_{H_2O} = 2.35$ kPa, measured by the impedance method.

LSSF conductivity rapidly weakens with increasing iron content and, already for a sample containing 3 at % Fe, the conductivities in dry and moist airs are almost identical. This means that the iron introduction decreases the proton conductivity of LSSF. These differences also decrease with increasing temperature due to a decrease in the $H_2O$ solubility (Fig. 5, inset; Fig. 7). This effect could be explained by a decrease in the water vapor solubility in LSSF due to a decrease in the oxygen vacancy concentration by reaction (5). Indeed, a strong decrease in the water vapor solubility in LSSF even at small iron additives was reported in [5]; however, this decrease in the solubility cannot be quantitatively explained by reaction (5).

### *3.6. Effect of the Atmosphere $p_{O_2}$ on the LSSF Conductivity*

The total conductivity of acceptor-doped oxide near its electrolytic region can be described by the known expression of three terms representing the ionic $\sigma_i$, electronic, and hole conductivities,

$$\sigma = \sigma_i + \sigma_n^0 p_{O_2}^{-1/4} + \sigma_p^0 p_{O_2}^{1/4}, \quad (6)$$

where $\sigma_n^0$ and $\sigma_p^0$ are constants. In this case, $\sigma_i$ is considered as the conductivity independent of $p_{O_2}$.

The conductivities of the LSSF samples under study appreciably decrease with lowering the partial oxygen pressure (Fig. 8), confirming the existence of the significant hole conductivity under oxidizing conditions according to reaction (3). For LSSF samples with 0–3 at % Fe additives, the conductivity in reducing atmospheres flattens, i.e., forms a horizontal plateau corresponding to the ionic conductivity $\sigma_i$, while

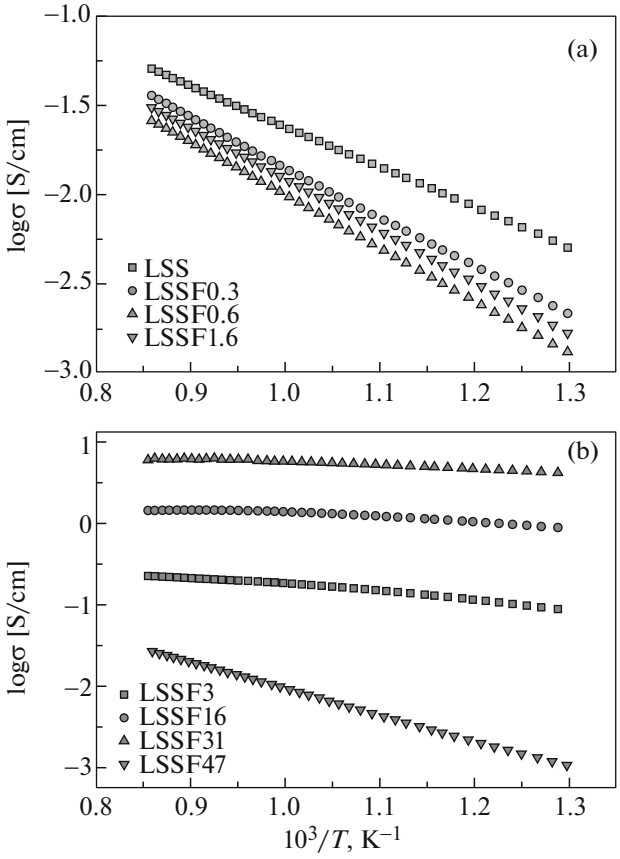


**Fig. 4.** Temperature dependences of the conductivity of samples of the LSSF system in moist air at $p_{H_2O} = 2.5$ kPa, measured by the four-probe method technique for (a) 0–1.6 at % Fe and (b) 3–47 at % Fe.

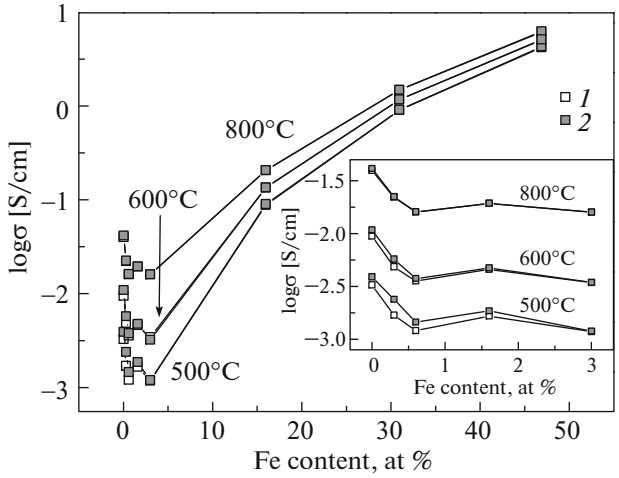


**Fig. 5.** Isotherms of the LSSF total conductivity in (*1*) dry ($p_{H_2O} = 0.04$ kPa) and (*2*) moist ($p_{H_2O} = 2.35$ kPa) air atmospheres as functions of the iron content at temperatures of 500, 600, and 800°C. The inset shows the range of small iron additives.

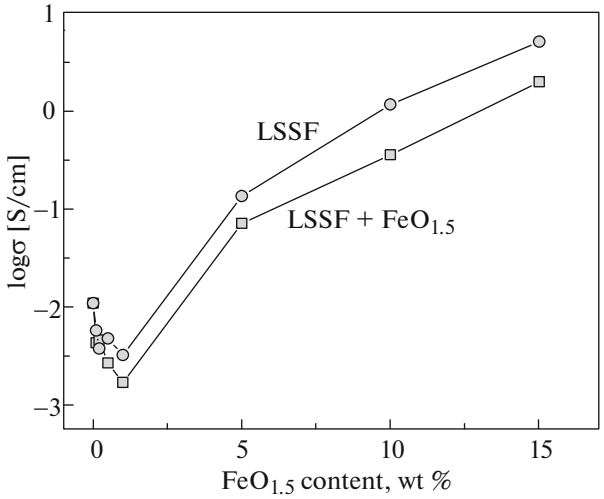


**Fig. 6.** Concentration dependences of the total conductivity of $La_{0.9}Sr_{0.1}Sc_{1-x}Fe_xO_{3-\alpha}$ and $La_{0.9}Sr_{0.1}ScO_{3-\alpha}$ + $FeO_{1.5}$ in terms of $FeO_{1.5}$ mass content at a temperature of 600°C in a moist air atmosphere ($p_{H_2O}$ = 2.35 kPa).

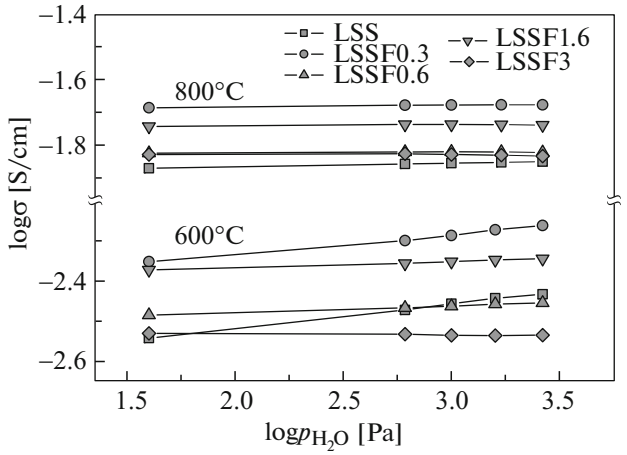


**Fig. 7.** Dependences of the total conductivity in the LSSF system with Fe contents of 0–3 at % in air on $\log(p_{H_2O})$ at temperatures of 600 and 800°C.

the hole conductivity is proportional to $p_{O_2}^{1/4}$ (Fig. 8). Since LSSF materials with small iron additives are ionic conductors in a reducing atmosphere, these experiments confirm the significant decrease in the ionic conductivity with iron concentration (Figs. 8 and 9), indicated above.

LSSF materials with significant iron additives (31 and 47 at % Fe) do not have a horizontal plateau in the case of a reducing atmosphere; concave curves are observed, which is caused by the superposition of three conductivity components according to Eq. (6). Equation (6) allows us to estimate the conductivities $\sigma_i$ for samples with iron contents of 16, 31, and 47 at % as $7 \times 10^{-4}$, $1.9 \times 10^{-3}$, and $6.8 \times 10^{-3}$ S/cm, respectively, at 800°C. The values obtained slightly differ from the minimum conductivity of samples in a reducing atmosphere and rapidly increase with iron concentration (Fig. 9). This clearly points to the fact that the quantity $\sigma_i$ is not purely ionic, but contains a large fraction of the electronic conductivity.

In a reducing atmosphere, the temperature dependences of the conductivity of LSSF31 and LSSF47 are almost strictly linear (Fig. 10) and have a high activation energy equal to 89 ± 1 kJ/mol. The temperature dependences of the conductivity of LSSFs with small (0.3–3 at %) Fe additives are *S*-shaped, as for the iron-free LSS sample (Fig. 10), which is a purely ionic conductor under these conditions [6]. The observed *S*-shape is a consequence of the superposition of two ionic conductivities, i.e., the low-temperature proton conductivity shaped as a curve with a maximum in the Arrhenius coordinates for all oxide protonics [15], and the high-temperature oxygen conductivity with high activation energy.

## 4. RESULTS AND DISCUSSION

The introduction of iron into LSS leads to an increase in the sample density, hence, the grain boundary density. However, the conductivity not only does not increase with iron content (0–3 at % Fe), but even decreases. In this case, the activation energy of the LSSF grain-boundary conductivity is significantly higher than the activation energy of the bulk conduc-

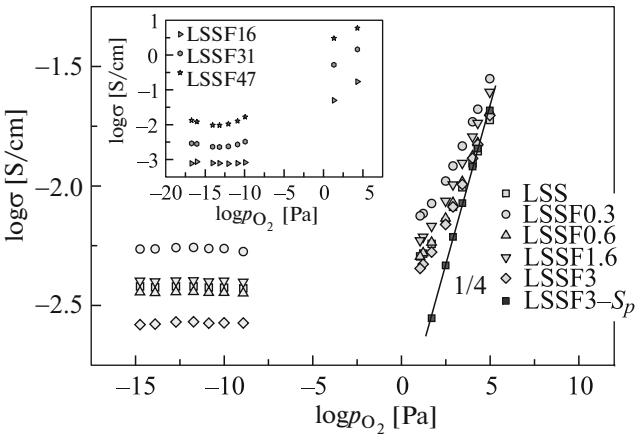


**Fig. 8.** Dependences of the total conductivity of LSSF samples containing from 0 to 3 at % Fe on the atmosphere $p_{O_2}$ at 800°C and $p_{H_2O}$ = 2.5 kPa. The dots in the straight line with a slope of 1/4 is the hole conductivity ($S_p$) of the LSSF3 sample. The inset shows the dependences of the total conductivity of LSSF16, LSSF31, and LSSF47 samples on $p_{O_2}$ under the same conditions.

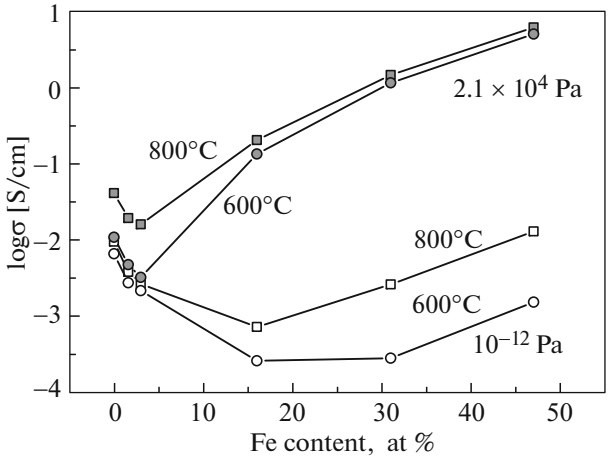


**Fig. 9.** Isotherms of the total conductivity as functions of the iron content in the LSSF system at $p_{H_2O} = 2.35$ kPa in a reducing atmosphere (open symbols) and in air (closed symbols) at temperatures of 600 and 800°C.

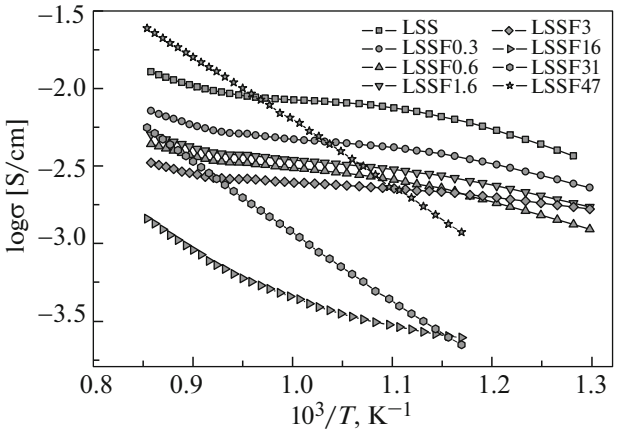


**Fig. 10.** Temperature dependences of the conductivity of samples of the LSSF system in a moist reducing atmosphere ($p_{O_2} = 10^{-12}$ Pa, $p_{H_2O} = 2.5$ kPa).

tivity (Fig. 3), which indicates the existence of the barrier for charge transfer through the grain boundary. It is most probable that the barrier appearance is associated with the change in the boundary region composition, which was experimentally shown for a number of perovskites in [16]. Indeed, in undoped $LaScO_3$, the intergrain resistivity is not observed [6, 8]. This becomes clear if we suppose that the grain-boundary barrier is formed due to compound ions concentrating at grain boundaries, which form a space charge similar to the double layer in electrochemical systems. However, cations in $LaScO_3$ have identical charges, and the oxygen sublattice does not contain oxygen vacancies.

However, a different situation arises when acceptor dopants (Sr, Mg) are introduced into $LaScO_3$. Increasing the bulk conductivity, such doping simultaneously leads to the high grain-boundary resistivity [6]. It is reasonable to assume that the grain-boundary resistivity is caused by the presence of alkaline-earth cations at grain boundaries. In the case of $La_{0.9}Sr_{0.1}ScO_{3-\alpha}$, strontium cations there will be at grain boundaries. The presence of strontium $Sr'_{La}$ with negative charge at grain boundaries will promote adsorption of iron $Fe^{\bullet}_{Sc}$ with positive effective charge at this boundary. $Fe^{4+}$ adsorption will result in a decrease in the number of oxygen vacancies at grain boundaries according to reaction (5), depleting the boundary region with protons and holes according to reactions (2) and (3), and will cause additional difficulties for transport of all carriers. Experiments confirm the decrease in the ionic, proton, and hole conductivity with increasing activation energy when introducing iron into LSS.

## 5. CONCLUSIONS

Single-phase ceramic samples $La_{0.9}Sr_{0.1}Sc_{1-x}Fe_xO_{3-\alpha}$ (where $x = 0$) with perovskite structure were synthesized by burning with ethylene glycol at 1400°C.

Isotherms of the total conductivity in a reducing atmosphere and in moist air ($p_{H_2O} = 2.35$ kPa) are shaped as curves with a minimum, since small iron additives (to 3 at % Fe) decrease the conductivity; large iron additives (16–47 at % Fe) increase it.

The bulk conductivity studied by the impedance method on LSSF samples (0.3–1.6 at % Fe) in the temperature range of 100–350°C has the activation energy $E_{act} = 48 \pm 1$ kJ/mol, which is higher than that of the grain-boundary conductivity by 1.5–2 orders of magnitude ($E_{act} = 70 \pm 1$ kJ/mol).

In a reducing atmosphere, LSSFs with small iron additives (to 3 at % Fe) exhibit properties of ionic conductors; LSSFs with large iron additives (16–47 at % Fe) are electronic semiconductors. Iron additives to 3 at % Fe almost completely suppress the proton conductivity, which prevents the use of LSSF materials as proton–electron membranes.

The negative effect of small iron additives on the LSSF conductivity was explained by $Fe^{4+}$ adsorption at grain boundaries enriched with strontium cations, which eventually complicates transport of all carriers through the boundary.

## ACKNOWLEDGMENTS

The authors are grateful to S.N. Plaksin for X-ray diffraction studies and E.Kh. Kurumchin, M.V. Kuimov, and E.P. Antonova for valuable remarks and discussion of the results.

This study was supported by the Russian Foundation for Basic Research (project no. 14-29-04013).

The analytical part of the study was performed using the equipment of the Shared Service Center "Composition of Materials" of the Institute of High-Temperature Electrochemistry of the Ural Branch of the Russian Academy of Sciences (Yekaterinburg, Russia).

## REFERENCES

1. H. Iwahara, Solid State Ionics **28–30**, 573 (1988).
2. K. D. Kreuer, Solid State Ionics **97**, 1 (1997).
3. B. Meng, Z. L. Lin, Y. I. Zhu, Q. Q. Yang, M. Kong, and B. F. Meng, Ionics **21**, 2575 (2015).
4. D. A. Medvedev, J. G. Lyagaeva, E. V. Gorbova, A. K. Demin, and P. Tsiakaras, Prog. Mater. Sci. **75**, 38 (2016).
5. D. Han, Y. Okumura, Y. Nose, and T. Uda, Solid State Ionics **181**, 1601 (2010).
6. V. P. Gorelov and A. Yu. Stroeva, Russ. J. Electrochem. **48** (10), 949 (2012).
7. A. Yu. Stroeva, V. B. Balakireva, L. A. Dunyushkina, and V. P. Gorelov, Russ. J. Electrochem. **46** (5), 552 (2010).
8. A. Yu. Stroeva and V. P. Gorelov, Russ. J. Electrochem. **48** (11), 1079 (2012).
9. A. Yu. Stroeva, V. P. Gorelov, and B. D. Antonov, Russ. J. Electrochem. **48** (12), 1171 (2012).
10. E. P. Antonova, D. I. Bronin, and A. Yu. Stroeva, Russ. J. Electrochem. **50** (7), 613 (2014).
11. V. B. Vykhodets, T. E. Kurennykh, O. A. Nefedova, V. P. Gorelov, A. Y. Stroeva, V. B. Balakireva, E. V. Vykhodets, and S. I. Obukhov, Solid State Ionics **263**, 152 (2014).
12. A. Yu. Stroeva, V. P. Gorelov, A. V. Kuz'min, V. G. Ponomareva, and S. A. Petrov, Phys. Solid State **57** (7), 1334 (2015).
13. S. Kemmler-Sack and I. Hofelich, Z. Naturforsch., B: Anorg. Chem., Org. Chem., Biochem., Biophys., Biol. **26** (6), 539 (1971).
14. http://abulafia.mt.ic.ac.uk/shannon/ptable.php.
15. K. D. Kreuer, Annu. Rev. Mater. Res. **33**, 333 (2003).
16. J. Druce, H. Téllez, M. Burriel, M. D. Sharp, L. J. Fawcett, S. N. Cook, D. S. McPhail, T. Ishihara, H. H. Brongersma, and J. A. Kilner, Energy Environ. Sci. **7**, 3593 (2014).

*Translated by A. Kazantsev*